

FACTA UNIVERSITATIS

Series: **Mechanical Engineering** Vol. 12, N° 1, 2014, pp. 37 - 50

Original scientific paper

## APPLICATION OF THE CRAIG-BAMPTON MODEL ORDER REDUCTION METHOD TO A COMPOSITE STRUCTURE: MAC AND XOR

UDC (531+624.01)

**Humberto Peredo Fuentes, Manfred Zehn**

Institute of Mechanics, Technical University Berlin, Germany

**Abstract** *The Craig-Bampton model order reduction (CBMOR) method based on the Rayleigh-Ritz approach is applied to dynamic behavior simulation of a composite structure in order to verify the method's feasibility and accuracy. The principle of this method is to represent a coupled component model based on the mass, damping and stiffness matrices. The methodology consists of a finite element model based on the classical laminate theory (CLT), a design of experiment to improve the modal assurance criteria (MAC) and experimental results in order to validate the reduced model based on CBMOR method and substructures (super-elements). Experimental modal analysis has been performed using a scanner laser Doppler vibrometer (SLDV) in order to assess the quality of the finite element models. The MAC and cross orthogonality MAC (XOR) values are computed to verify the eigenfrequencies and eigenvectors. This approach demonstrates the feasibility of using CBMOR for composite structures. The example is prepared and solved with MSC/NASTRAN SOL103. The design of experiments (DOE) method has been applied in order to identify the critical parameters and thus obtain high MAC values.*

**Key Words:** *SDDTools-MATLAB, NASTRAN, Modal Analysis, Composites*

### 1. INTRODUCTION

Many techniques have been proposed to obtain reduced order finite element models (known as model order reduction (MOR) methods) by reducing the order of mass and stiffness matrices of structures made of conventional materials [1-3]. The substitution of conventional materials by composite materials in the aeronautic, space and automotive industry is becoming increasingly important today for the production of industrial high-performance components [11-13]. The state-of-the-art MOR techniques are classified in

---

Received November 27, 2013 / Accepted February 4, 2014

**Corresponding author:** Humberto Peredo Fuentes

Technical University Berlin, Institute of Mechanics, Berlin, Germany

E-mail: hperedo@mailbox.tu-berlin.de

four groups [19]: direct reduction, modal methods, reduction with Ritz vectors and the component mode synthesis (CMS). According to this classification, the last two groups yield the best results. The Ritz vectors improve the accuracy-cost ratio and the CMS combines the first three classes of methods. Hence the MOR method based on the Rayleigh-Ritz approach is used to improve the accuracy-time ratio in civil and aeronautical engineering applications in many areas of structural dynamics [6, 14, 19, 22, 23]. Thus, it is necessary to study the feasibility and efficiency of using the CMS with the Rayleigh-Ritz reduction basis in order to describe the dynamic behavior of a composite structure [14, 19]. The sections 2-4 introduce to MOR based on the Ritz vectors, classical CMS and substructures, respectively. The classical laminate theory (CLT) is introduced in Section 5. Sections 6-8 demonstrate a sensitivity analysis performed by using different tools – design of experiment (DOE), finite element method (FEM) and modal assurance criteria (MAC).

## 2. MODEL ORDER REDUCTION WITH RITZ VECTORS

It is typical for coupled problems with model sub-structuring [6, 14, 22, 23] to have an accurate second order representation in the form:

$$\begin{aligned} ([M]s^2 + [C]s + [K])\{q\} &= [b]\{u\} \\ \{y\} &= [c]\{q\} \end{aligned}, \quad (1)$$

where  $s$  is the Laplace variable,  $[M]$ ,  $[C]$ ,  $[K]$  are mass, damping and stiffness matrices, respectively,  $\{q\}$  are generalized degrees of freedom (DOFs),  $[b]$  and  $[c]$  are input and output matrices, respectively,  $\{u\}$  are the inputs describing the time/frequency dependence, and  $\{y\}$  are the physical outputs.

In this description, two - not very classical and yet important - assumptions are made:

- 1) The decomposition of discretized loads  $F(s)$  as the product of the fixed input shape matrix specifying the spatial localization of loads  $[b]$  and inputs  $\{u\}$ .
- 2) The definition of physical outputs  $\{y\}$  is a linear combination of DOFs  $\{q\}$ .

The Ritz/Galerkin displacement methods seek approximations of the response within a subspace characterized by matrix  $[T]$  associated with generalized DOFs  $\{q_R\}$ :

$$\{q\} = [T]\{q_R\}, \quad (2)$$

where  $\{q\}$  is the original set of DOF and  $\{q_R\}$  is the reduced set of DOF, substituting Eq. (2) into Eq. (1) leading to an overdetermined set of equations. The Ritz approximation assumes that the virtual work of displacements in the dual subspace generated by  $[T]^T$  is also zero, thus leading to a reduced model:

$$\begin{aligned} ([T]^T[M][T] \quad s^2 + [T]^T[C][T] \quad s + [T]^T[K][T]) \quad \{q_R(s)\} &= [T]^T[B] \{u(s)\} \\ \{y(s)\} &= [c][T] \{q_R(s)\} \end{aligned}. \quad (3)$$

### 3. CLASSICAL CMS BASES AS APPROXIMATION OF THE FREQUENCY RESPONSE

The method was first developed by Walter Hurty in 1964 [1] and later expanded by Roy Craig and Mervyn Bampton [2] in 1968. Component mode synthesis and model reduction methods provide for the means for building appropriate  $[T]$  bases (the subspace spanned rectangular matrix). There are many ways of proving classical bases [22]. Their validity is associated with two assumptions: the model needs to be valid over a restricted frequency band and the number of inputs is limited. One needs to translate this hypothesis into the requirement to include mode shapes and static responses into  $[T]$  basis. Most of the literature on CMS implies the fundamental assumption for coupling, which states that the displacement is continuous at the interfaces. Considering the response of an elastic structure to applied loads  $F(s)=[b]\{u(s)\}$ , the exact response at a given frequency  $[H(s)]$  is given by:

$$[H(s)] = [c]\{[M]s^2 + [K]\}^{-1}[b] = [c][Z(s)]^{-1}[b], \quad (4)$$

where  $[Z(s)]$  is the dynamic stiffness. If there is no external excitation:

$$[Z(\lambda_j)]^{-1}\{\phi_j\} = \{0\}, \quad (5)$$

and the solutions are known as free modes of the structure, where  $\lambda_j$  is  $j^{\text{th}}$  eigenvalue of the matrix and  $\{\phi_j\}$  is  $j^{\text{th}}$  eigenvector. A reduction model should include these shapes to allow for an accurate representation of the resonances which are associated with the singularities of the dynamic stiffness. A point of particular interest is the static response at  $s=0$ . The associated deformation is:

$$\{q(s=0)\} = [Z(0)]^{-1}[b]\{u(0)\} = [T_s]\{u(0)\}. \quad (6)$$

The columns of  $[T_s]$  are also called attachment modes [22]. For the case of free floating structures (structures with rigid modes),  $[Z(0)]$  is singular and one defines attachment modes as responses of all modes except for the rigid body modes.

The bases combining free modes and attachment modes are valid over a certain frequency range (truncation of the series of free modes) and certain inputs characterized by  $[b]$ .

One, thus, considers the response of the structure with enforced displacements on a subset of DOFs. Division of the DOFs in two groups – active or interface DOFs denoted by  $I$  in the subscript, and complementary, denoted by  $C$  in the subscript, leads to:

$$\begin{bmatrix} [Z_{II}(s)] & [Z_{IC}(s)] \\ [Z_{CI}(s)] & [Z_{CC}(s)] \end{bmatrix} \begin{Bmatrix} \langle \{q_I(s)\} \rangle \\ q_C(s) \end{Bmatrix} = \begin{Bmatrix} R_I(s) \\ \langle \{0\} \rangle \end{Bmatrix}, \quad (7)$$

where  $\langle \{q_I(s)\} \rangle$  and  $\langle \{0\} \rangle$  denotes a known quantity. The exact solution to this problem is:

$$\{q\} = [T(s)]\{q_I\} = \begin{bmatrix} [I] \\ -[Z_{CC}(s)]^{-1}[Z_{CI}(s)] \end{bmatrix} \{q_I\}. \quad (8)$$

The subspace found here is frequency dependent and can only be used in very restricted applications [23]. A classical approximation is to evaluate the static ( $s=0$ ) value in this subspace for the active or interface DOFs denoted by  $CI$  in the subscript, and complementary,  $CC$  in the subscript:

$$[T] = \begin{bmatrix} [I] \\ [-K_{CC}]^{-1}[K_{CI}] \end{bmatrix}. \quad (9)$$

Reduction on this basis is known as static or Guyan condensation [4]. The columns of  $[T]$  are called constraint modes [22]. They correspond to unit displacements of the interface DOFs. Significant deviations can be expected when  $[Z_{CC}(s)]^{-1}$  differs from  $[Z_{CC}(0)]^{-1}=[K_{CC}]^{-1}$ . Such difference is significant for singularities of  $[Z_{CC}(s)]^{-1}$  which are computed by the eigenvalue problem:

$$\begin{bmatrix} [0] & [0] \\ [0] & [Z_{CC}(\omega_j)] \end{bmatrix} \begin{Bmatrix} 0 \\ \phi_{j,c} \end{Bmatrix} = 0. \quad (10)$$

The use of a basis combining constraint, Eq. (9), and fixed-interface modes, Eq. (10), is proposed in [2]. It yields the Craig-Bampton method:

$$[T] = \begin{bmatrix} [I] & [0] \\ [-K_{CC}]^{-1}[K_{CI}] & [\phi_{NM,C}] \end{bmatrix}, \quad (11)$$

where  $[\phi_{NM,C}]$  is the interior part of the matrix of kept fixed-interface modes. There are many results reported by Balmès *et al.* [6, 14, 15] obtained by the Craig-Bampton model order reduction (CBMOR) and the Rayleigh-Ritz vectors approach in order to solve coupled problems related to model sub-structuring (also known as component mode synthesis).

One should be aware of the fact that the use of Raleigh-Ritz vectors leads to dense matrices, as opposed to not reduced FEM models characterized by a sparse form of the matrices.

#### 4. SUBSTRUCTURES OR SUPER-ELEMENTS

Sub-structuring is a procedure that condenses a group of finite elements into one element. It implies that the whole structure is divided into smaller structures (see Figs. 1 and 2), and the resulting elements are referred to as super-elements. In the considered case (Fig. 1), the structure is divided into two substructures using 123 nodes at the interface. The model size is reduced from 37,698 DOF to 579 DOF.

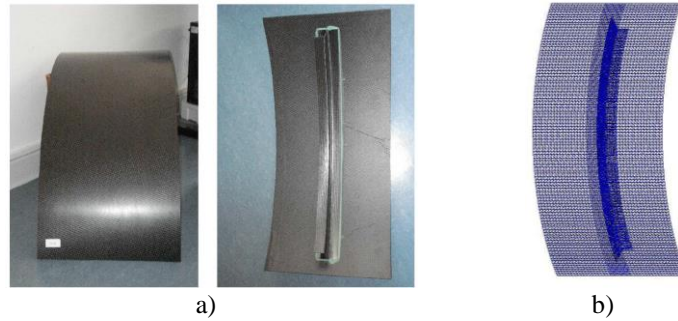


**Fig. 1** Prototype and FEM model in NASTRAN and SDTools:  
a) Composite structure – front and back; b) FEM model

The basic sub-structuring idea is to consider a part of the model separately and extract the degrees of freedom needed to connect this part to the rest of the model. Therefore, the result of sub-structuring is a collection of finite elements whose response is defined by the stiffness and mass of the retained degrees of freedom. The categories of modal truncation sub-structuring and static condensation approaches have been widely applied relying on the eigenfrequency information [3, 23].

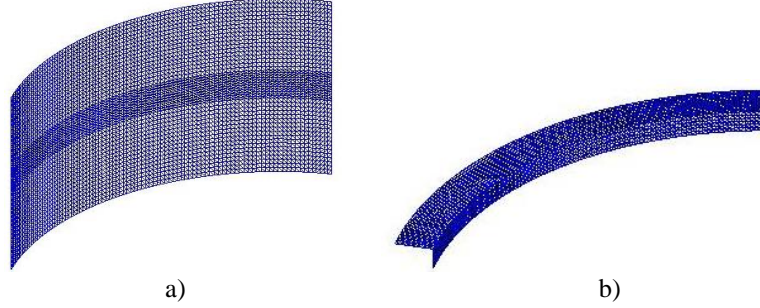


**Fig. 2** Sub-structuring: a) Substructure 1; b) Substructure 2

## 5. LAMINATE THEORY

The classical laminate theory is applicable to linear and composite elastic materials [21] by means of the Discrete Kirchhoff Theory (DKT) elements [20]. The CLT has been used extensively to predict elastic behavior of the traditional fiber-reinforced polymers (FRP). FRP materials (carbon or glass FRP) are widely used in aerospace and construction applications. One important consideration is to have perfectly bonded layers with a uniform thickness (see Fig. 3). The mechanical properties measured in ply level experiments are used to populate the stiffness matrix for each ply. The stiffness matrices for the individual plies are combined to form the laminate stiffness matrix – the ABC matrix:

$$\begin{pmatrix} N_x \\ N_y \\ N_{xy} \\ M_x \\ M_y \\ M_z \end{pmatrix} = \begin{pmatrix} A & B \\ B & C \end{pmatrix} \times \begin{pmatrix} \varepsilon_x \\ \varepsilon_y \\ \gamma_{xy} \\ \kappa_x \\ \kappa_y \\ \kappa_{xy} \end{pmatrix}. \quad (6)$$

The ABC matrix relates forces ( $N_i$ ) and moments ( $M_i$ ) to strains ( $\varepsilon_i$ ) and curvatures ( $\kappa_i$ ). The components of the ABC matrix are given in Eqs. (7-9), where  $N$  is the number of plies,  $Q_k$  is the stiffness matrix of each ply, and  $Z_k$  denotes the distance from the laminate's mid-plane to the edges of single plies:

$$A = \sum_{k=1}^N Q_k \times [Z_k - Z_{k-1}], \text{ in-plane stiffness matrix,} \quad (7)$$

$$B = \frac{1}{2} \sum_{k=1}^N Q_k \times [Z_k^2 - Z_{k-1}^2], \text{ bending-stretching coupling matrix,} \quad (8)$$

$$C = \frac{1}{3} \sum_{k=1}^N Q_k \times [Z_k^3 - Z_{k-1}^3], \text{ bending-stiffness matrix.} \quad (9)$$

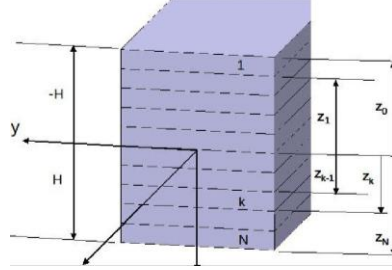


**Fig. 3** Configuration of composite layers

The prototype and the finite element (FE) model are shown in Fig. 1. The composite structure incorporates three parts (properties in Table 1). The first component is made of Hunts-man Ly 564 + Hexcel Gewebe G0926 (HTA-Faser) with dimensions of 0.390m  $\times$  0.810m (Fig. 2). The middle shell that connects the two principal parts (Fig. 2a) has dimensions of 0.710m  $\times$  0.030m. Finally, there is the C-section Hexcel RTM6 + Saertex Multi-Axial-Gelege (MAG) with a IM7-Faser with dimensions of 0.710m  $\times$  0.030m. All the parts have symmetric layer distribution [45/-45/45/-45]<sub>s</sub>.

## 6. DESIGN VIA FINITE ELEMENT ANALYSIS (FULL AND REDUCED MODEL)

Our study is divided into two parts.

The first part is a full modal analysis using the same model but with two different solvers for reference purposes. Two types of elements have been used: CTRIA3 shell (from MSC/NASTRAN) and PSHELL (from SDTools).

The second part is setting the reduced model by using SDTools for MATLAB. The reduced model is built up defining two super-elements. Super-element 1 (Fig. 2a) has 4,753 nodes and 9,219 elements, while super-element 2, (Fig. 2b) has 1,615 nodes and 3,026 elements. The defined super-elements share 579 DOF distributed in 123 nodes along the common border with different DOF per node, according to the CMS that has defined an appropriate  $[T]$  matrix, used in [3]. We have calculated the same number of modes in each super-element and performed a cross orthogonality MAC (XOR) evaluation to verify the approximation of the MOR used in low (12 mode pairs) and/or high frequency range (29 mode pairs) versus the full model.

In order to estimate the main parameters (qualitative and quantitative) that affect our MOR based on the number of substructures and nodes, we have performed a DOE using first the full model and the experimental analysis. The DOE study is performed using the methodology implemented in Minitab 16 [7]. Fig. 4a shows the main effects of each parameter in the composite structure based on the physical characteristics selected. The

main effect is identified through the slope generated due to the eigenfrequency values between the limits defined for each parameter – a bigger slope means a strong parameter effect. Due to the number of parameters, it is necessary to perform first a DOE-screening with  $2^{10-5}=32$  "runs" and then a full factorial with the identified principal parameters based on the DOE-screening.

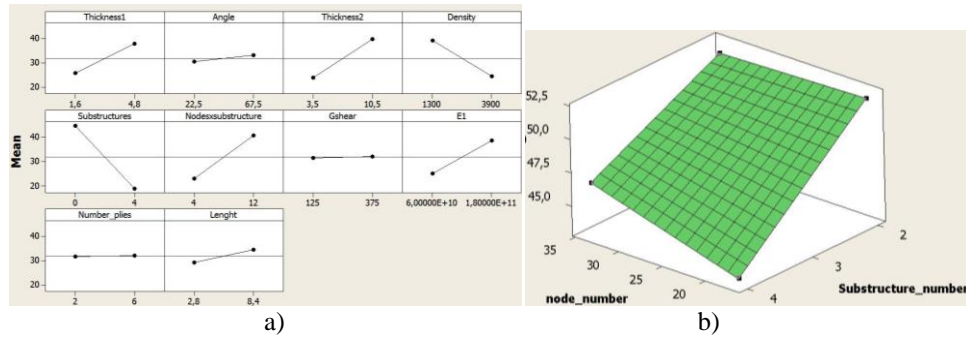


**Fig. 4** DOE: a) Parameters main effects, b) Surface response

The results shown in Fig. 5a (vertical left side) are eigenfrequencies. The MAC correlation between the full model and experimental data help us validate the MOR results. The Young Modulus, density, number of nodes and substructure parameters have a strong influence reflected in the slope (Fig. 4b) and in the MAC values (section 7). Once we have selected the main parameters based on the DOE-screening, we perform a DOE full factorial  $2^4$  and obtain a surface response (see Fig. 4b) that help us find the best model for the parameter limits selected. This process is known in literature as updating. Jing [8], Barner [9] and Xiaoping *et al.* [10] reported the use of design of experiments in order to quantify and qualify different key parameters in mechanical components (stresses, displacements, low and high cycle fatigue, and frequencies). The DOE is a sensitivity analysis tool used to estimate the critical input parameters.

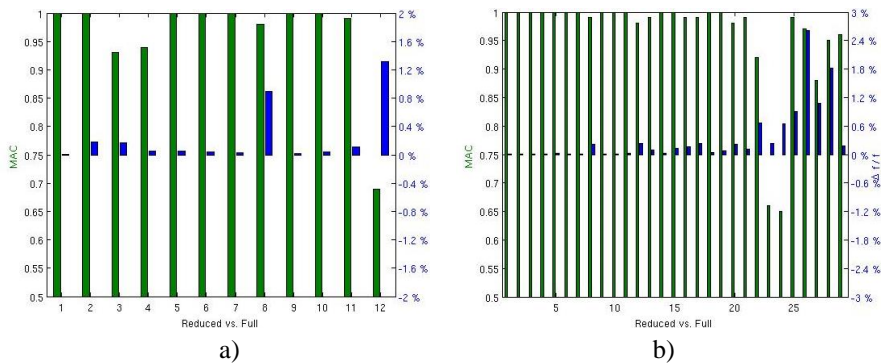


**Fig. 5** Cross orthogonality MAC reduced vs. full model: (a) low frequencies (b) higher frequencies (green bars MAC, blue bars frequency difference)

In Fig. 5, we can see the low and high mode pairs selected between the full and reduced model (12 and 29 mode pairs), respectively. The green bars show the eigenvector criteria and the blue bars the eigenfrequency difference between the reduced and the full model. The low frequencies show a larger difference in the 3<sup>rd</sup>, 4<sup>th</sup> and 12<sup>th</sup> mode pair. The largest difference in the frequencies is about 1.2% (low eigenfrequencies) between the full and reduced model. Increasing the number of pairs, the eigenfrequency difference increases up to 3% for 29 pairs. However, the mode pairs 3, 4 and 12 have improved suggesting that the accuracy using CBMOR method depends on the number of retained constraint modes. Most of the pair selections have a correlation above 90%, except for the 12<sup>th</sup> mode pair in the low frequency range and the 23<sup>rd</sup> and 24<sup>th</sup> pair in a high frequency range. Table 2 shows the values comparing the full with a reduced model for low frequency. A 3D plot of the XOR for high frequency pairs is given in Fig. 6.

**Table 1** Orthotropic elastic mechanical properties per thickness

Modulus	Th <sub>1</sub> (m)	E(GPa)	$\nu(-)$	Shear	G(GPa)	$\rho(\text{Kgm}^{-3})$
E <sub>1</sub>	0.035	71.3	0.3	G1	7.0	2600
E <sub>2</sub>		97.3	0.3	G2	5.0	
				G3	7.0	
Modulus	Th <sub>2</sub> (m)	E(GPa)	$\nu(-)$	Shear	G(GPa)	$\rho(\text{Kgm}^{-3})$
E <sub>1</sub>	0.007	71.3	0.2	G1	6.0	1500
E <sub>2</sub>		68.3	0.2	G2	5.0	
				G3	6.0	
Modulus	Th <sub>3</sub> (m)	E(GPa)	$\nu(-)$	Shear	G(GPa)	$\rho(\text{Kgm}^{-3})$
E <sub>1</sub>	0.035	71.3	0.2	G1	6.0	1500
E <sub>2</sub>		68.3	0.2	G2	5.0	
				G3	6.0	

**Table 2** MAC values: full versus CBROM reduced model

#	Full	#	Reduced	DF/FA	MAC
7	57.218	7	57.218	0.0	100
8	106.02	8	106.21	0.2	100
9	167.50	9	167.79	0.2	93
10	168.2	10	168.29	0.1	94
11	234.99	11	235.12	0.1	100
12	236.83	12	236.93	0.0	100
13	315.26	13	315.33	0.0	100
14	323.93	14	326.82	0.9	98
15	401.72	15	401.77	0.0	100
16	408.39	16	408.57	0.0	100
17	432.89	17	433.39	0.1	99
18	494.90	18	501.41	1.3	69

The correlation of nearly double modes 9-10,11-12,13-14 and 15-16 in Table 2 suggests the possibility of having bending and torsional modes at close frequencies in the composite structure (mode veering) [24]. Thus, a lower MAC value is expected in some mode pairs in the experimental validation. There are only three types of structures made of



the conventional materials that have been identified to exhibit veering: symmetric or cyclic structures, multi-dimensional structures such as plates having bending and torsion at close frequencies and structures with fully uncoupled substructures. The considered structure corresponds to the second type – multi-dimensional plate structures.

## 7. MODAL ASSURANCE CRITERION (MAC)

There are two general categories for correlation criteria: eigenfrequencies and eigenvectors [18]. The MAC is one of the most useful comparison methods that relies on the eigenvector information according to Eq. (10). The MAC is a known vector correlation between the experimental and the FE model. To approximate the measurements through a polynomial function, (Fig. 9), we use the frequency domain identification of structural dynamics applying the pole/residue parameterization [15].

$$MAC(i) = \frac{\left( \sum_{j=1}^l (c_j \varphi_{id})^H (c_j \varphi_k) \right)^2}{\sum_{j=1}^l (c_j \varphi_{id})^H (c_j \varphi_{id}) \sum_{j=1}^l (c_j \varphi_k)^H (c_j \varphi_k)} \quad (10)$$

The MAC value of 100 % corresponds to an absolute correlation. The less this value becomes, the worse the eigenvector correlation is ( $c_j \varphi_{id}$  is the  $j^{\text{th}}$  mode shape at sensors and  $c_j \varphi_k$  is the  $j^{\text{th}}$  analytical mode shape), provided that the observability law for the selection of DOFs is not violated. A MAC coefficient of a magnitude larger or equal than 90% implies a satisfactory correlation. In Fig. 8, we observe some mode shapes of the reduced and full models. Figs. 10a, 10b, and 10c, show the MAC between the full and the experimental measurements in MATLAB, NASTRAN, and CBMOR model, respectively. The correlation is performed for a low frequency range (up to 400 Hz), based on the fitting model generated from the experimental measurements [3, 15].

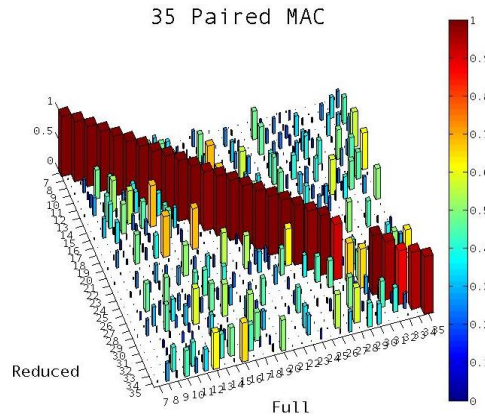


**Fig. 6** Cross orthogonality MAC (XOR): higher frequencies – reduced vs. full model

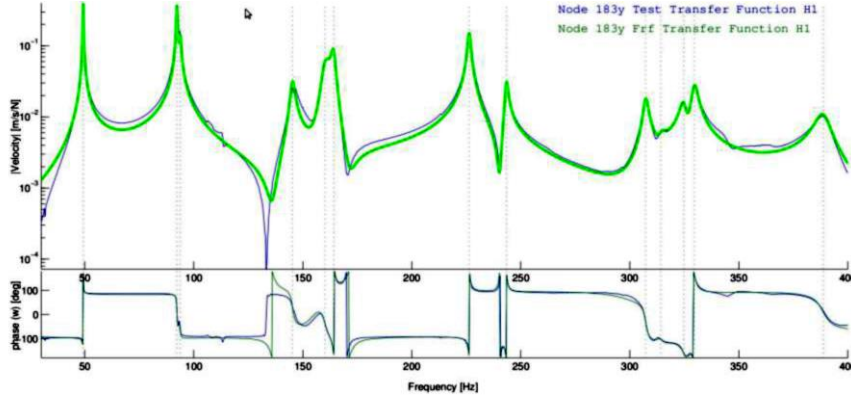


Fig. 7 FRF(blue) and fitting curve (green) of composite model at node 183y

## 8. EXPERIMENTAL MODAL ANALYSIS

All the measurements are performed with the Scanning Laser Doppler Vibrometer (SLDV) PSV 840 (Fig. 9a). It is a complete and compact system including a sensor head, a PC with DSP boards and Windows NT-based application software packages [16]. Discrete Fourier transform is applied to response  $x(t)$  and excitation  $f(t)$  to give  $X(\omega_i)$  and  $F(\omega_i)$ , respectively [17]. The frequency response function (FRF),  $H(\omega_i)$ , is defined as the ratio of the transformed excitation [18]:

$$H(\omega_i) = \frac{X(\omega_i)}{F(\omega_i)}, \quad (11)$$

where  $H(\omega_i)$  is the identified (predicted) FRF transfer function matrix,  $H(\omega_i)$  the measured FRF transfer function matrix,  $X(\omega_i)$  the Fourier spectrum of response, and  $F(\omega_i)$  is the Fourier spectrum of excitation force. The FRF in Eq. (11) is the inverse of the dynamic stiffness matrix:

$$H(\omega_i) = [-\omega_i^2 [M] + \omega_i [C] + [K]]^{-1}. \quad (12)$$

Mass  $[M]$ , damping  $[C]$  and stiffness  $[K]$  matrices in Eq. (12) are dependent on physical parameters such as material's density, Young's and shear moduli and Poisson ratio.

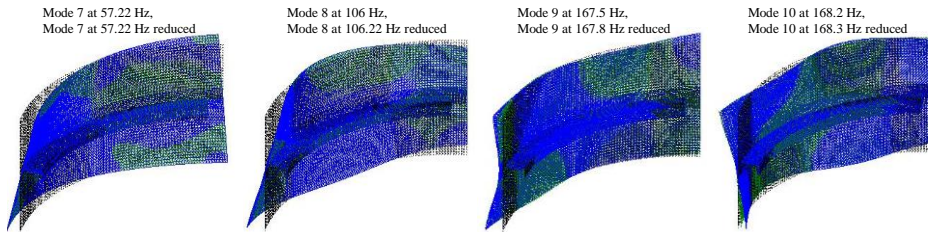
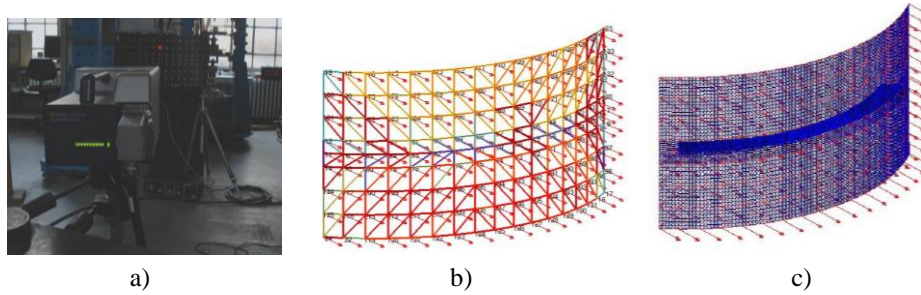


Fig. 8 CBMOR (in green) vs full model in MATLAB (in blue)



**Fig. 9** Experiment: a) Experimental set-up; b) 153 Y-direction sensors; c) 153 sensors in the FEM model

The SLDV employs a laser to sweep over the structure continuously while measuring, capturing the response of the structure from a moving measurement point. Various methods have been devised to determine the mode shapes of the structure everywhere along the scan path measurement [16]. A bandwidth of 2% is used in order to localize the eigenfrequencies. The composite structure has rather small internal damping and the experimental modal analysis below 400 Hz is performed. The structure is excited by means of a shaker at node 17 (Fig. 9a and Fig. 9b) that is located in the right bottom corner. The input force is measured using a force transducer type 8200 in combination with a charge to CCLD converter Type 2646 in order to record the excitation in the transverse direction.

The interpolation between the experimental measurements uses Frequency Response Functions (FRF) [15], (Fig. 7). The FRFs allow comparison of the experimental modal parameters (frequency, damping, and mode shape) with those of the FE model. The Fast Fourier Transform (FFT) is a fundamental procedure that isolates the inherent dynamic properties of a mechanical structure and in our case with respect to the full and reduced FE model. The MAC analysis (Fig.10) shows a high correlation between the full model, the reduced model and the experimental measurements. The nearly double correlation in the experimental results identified in Table 3 (previously identified applying the CBMOR method in Table 2), suggests the presence of the veering phenomena (bending and torsional mode at the same frequency) in the considered composite structure. This is reflected in the MAC values for the corresponding modes.

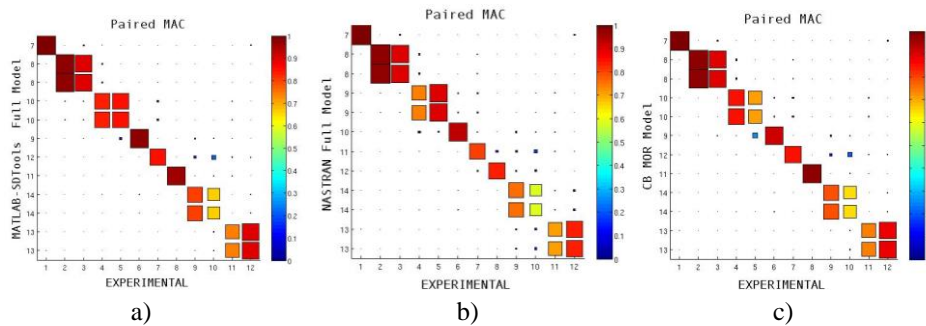


**Fig. 10** Comparative MAC: a) SDtools-Exp, b) MSC/NASTRAN-Exp, c) CBMOR-Exp

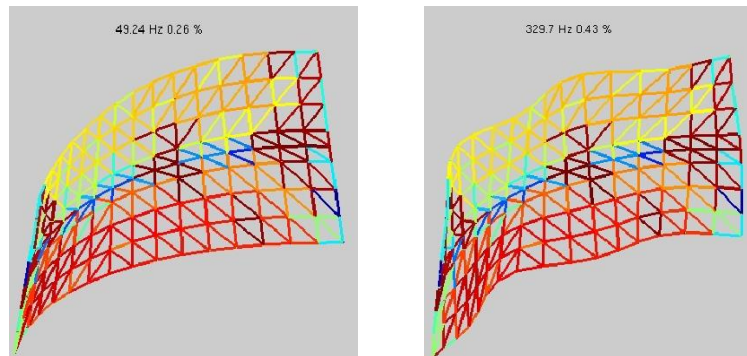


**Fig. 11** Experimental mode shapes

Pierre [25] reported how localization and veering are related to two kinds of "coupling": the physical coupling between structural components, and the modal coupling set up between mode shapes through parameter perturbations.

His studies show that, in structures with close eigenvalues, small structural irregularities (could be our case) result in both strong localization of modes and abrupt veering away of the loci of the eigenvalues when these are plotted against a parameter representing the system disorder. The study of the presence of this phenomenon in the composite structure is beyond the scope of this work.

Table 3 shows the MAC values obtained for each case between the full and reduced model versus the experimental results. The mode shapes depicted in Fig. 11 are the experimental results.

**Table 3** Full and reduced FEM model results versus experimental results

#	Experimental	#	Full	DF/FA	MAC	CBMOR	DF/FA	MAC
1	49.243	7	57.218	16.2	100	57.218	16.2	100
2	92.265	8	106.02	14.9	97	106.21	15.1	97
3	93.756	8	106.02	13.1	90	106.21	13.3	90
4	145.29	10	168.20	15.8	83	168.29	15.8	84
5	160.05	10	168.20	5.1	86	168.29	5.1	71
6	164.18	9	167.50	2.0	98	167.79	2.2	92
7	226.36	12	236.83	4.6	86	236.93	4.7	85
8	243.40	11	234.99	-3.5	96	235.12	-3.4	97
9	307.33	14	323.93	5.4	81	326.82	5.4	80
10	314.18	14	323.93	3.1	66	326.82	4.0	65
11	324.83	13	315.26	-2.9	74	315.33	-2.9	74
12	329.67	13	315.26	-4.4	90	315.33	-4.3	89

## 9. CONCLUSIONS

The results have shown a good correlation in dynamic behavior of the composite structure model using the DKT elements with different solvers. The MAC values with the full and reduced models have also shown a good agreement with the experimental results. In order to achieve high quality models that can adequately capture the dynamic behavior, the material properties are updated through the DOE and are crucial in the MOR correlation with the experimental results. The updated mass and stiffness matrices in the full model play an important role in this procedure. Furthermore, the reduced model obtained by means of the Craig-Bampton MOR method (the reduced model couples 2 substructures through 123 nodes and 579 DOF) has demonstrated a good agreement with the experimental results. The MAC values for the FEM models as well with the experimental results suggest a presence of mode veering phenomenon (bending and torsional mode at the same frequency in the considered composite structure). And finally, the experimental results using a SLDV as well as the identification of pole/residues used in [15], are suitable to validate the dynamic analysis using modal order reduction. It is improper to draw conclusions from a single example, but the obtained results using two different solvers are coherent. This conducted work obviously leaves much room for further research. Other modal assurance criteria need to be performed, such as coordinate modal assurance criteria (COMAC), enhanced modal assurance criteria (ECOMAC) and scale coordinate assurance criteria (S-COMAC) and also other model order reduction and/or mode shape expansion methods should be assessed.

## REFERENCES

1. Hurty, W. C., 1965, *Dynamic analysis of structural systems using component modes*, AIAA Journal, 3(4), pp. 678-685.
2. Craig R. J. and Bampton M., 1968, *Coupling of substructures for dynamic analyses*, AIAA Journal 6(7), pp.1313-1319.
3. SDTools Inc. 2011, *Structural dynamics toolbox and FEMLink, User's Guide*, SDTools, Ver. 6.4, Paris, France.
4. Guyan, J. 1965, *Reduction of stiffness and mass matrices*, AIAA Journal, 3(380), pp.
5. Irons, B. M., 1965, *Structural eigenvalue problems - elimination of unwanted variables*, AIAA Journal, 3(5): pp. 961-962.
6. Balmès E., 1996, *Use of generalized interface degrees of freedom in component mode synthesis*, International Modal Analysis Conference, pp. 204-210.
7. Montgomery, D. C., 2000, *Design and analysis of experiments*, John Wiley & Sons.
8. Fan J., Zeng, W., Wang R., Sherr X., Chen Z., 2010, *Research on design and optimization of the turbine blade shroud*, 2<sup>nd</sup> International Conference on Engineering Optimization, Lisbon, Portugal.
9. Barner, N., 2010, *iSight-Abaqus optimization of a ring-stiffened Cylinder*, SIMULIA Customer Conference.
10. Chen, X., Yu, X., and Ji B., 2010, *Study of crankshaft strength based on iSIGHT platform and DOE methods*, International Conference on Measuring Technology and Mechatronics Automation, pp. 548-551.
11. Lauwagie, T., 2005, *Vibration-Based Methods for the Identification of the Elastic Properties of Layered Materials*, PhD thesis, Catholic University of Leuven, Belgium.
12. Reddy, J. N., 2005, *Mechanics of Laminated Composite Plates and Shells Theory and Analysis*, CRC, Press Second edition.
13. Berthelot, J. M., 1992, *Materiaux composites: Comportement mecanique et analyse des structures*, Lavoisier, Paris, France
14. Balmès E., 1997, *Efficient Sensitivity Analysis Based on Finite Element Model Reduction*, International Modal Analysis Conference, IMAC, pp.1-7.
15. Balmès E., 1996, *Frequency domain identification of structural dynamics using the pole/residue parametrization*, International Modal Analysis Conference, pp. 540-546.

16. Gade, S., Møller, N.B., Jacobsen, N.J., and Hardonk, B., 2000, *Modal analysis using a scanning laser Doppler vibrometer*, Sound and Vibration Measurements, pp. 1015-1019.
17. Newland, D.E., 1993, *An Introduction to random vibration, spectral and wavelet Analysis*, New York, Longman, Harlow and John Wiley.
18. Ewings, D. J., 1995, *Modal testing: Theory and practice*, Research Studies Press, Letchworth, United Kingdom.
19. Cunedioğlu, Y., Muğan, A., Akçay, H., 2006, *Frequency domain analysis of model order reduction techniques*, Finite Elements in Analysis and Design, 42, pp. 367-403.
20. Batoz, J.L., Bathe, K.J., Ho, L.W., 1980, *A Study of three node triangular plate bending elements*, International Journal for Numerical Methods in Engineering, 15, pp. 1771-1812.
21. Batoz, J.L., Lardeur, P., 1989, *Composite plate analysis using a new discrete shear triangular finite element*, International Journal for Numerical Methods in Engineering, 27, pp. 343-359.
22. Craig, R.J., 1987, *A review of time-domain and frequency domain component mode synthesis methods*. Int. J. Anal. and Exp. Modal Analysis, 2(2), pp. 59-72.
23. Balmès, E., 2000, *Review and Evaluation of shape expansion methods*, International Modal Analysis Conference, pp. 555-561.
24. Bonisoli E, Delprete C., Esposito M., Mottershead J. E., 2011, *Structural Dynamics with coincident Eigenvalues: Modeling and Testing*, Modal Analysis Topics 3, pp 325-337.
25. Pierre C., 1988, *Mode Localization and eigenvalue loci of Bridges with Aeroelastic effects*, Journal of Engineering Mechanics 126(3), pp. 485-502.

## **PRIMENA CRAIG-BAMPTON REDUKCIJE MODELA NA STRUKTURU OD KOMPOZITNOG MATERIJALA: MAC I XOR**

*Craig-Bampton metoda za redukciju modela (CBMOR) zasnovana na Rayleigh-Ritz pristupu je primenjena u simulaciji dinamičkog ponašanja kompozitnih struktura u cilju verifikacije izvodljivosti i tačnosti ove metode. Princip ove metode je da predstavi model spregnutih komponenti preko matrica inercije, prigušenja i krutosti. Metodologija uključuje model primenom konačnih elemenata (MKE) na osnovu klasične teorije laminata (CLT), zatim postavku eksperimenta sa ciljem poboljšanja vrednosti koeficijenata poređenja modova (MAC), kao i eksperimentalne rezultate sa ciljem validacije redukovanog modela primenom CBMOR metode i substrukture (superelemenata). Eksperimentalna modalna analiza je sprovedena korišćenjem laserskog Doplerovog vibrometra da bi se ocenio kvalitet MKE modela. MAC vrednosti za pripadajuće i nepripadajuće modove su sračunate da bi se verifikovale sopstvene frekvence i modovi. Ovaj postupak pokazuje izvodljivost primene CBMOR redukcije modela u slučaju kompozitnih struktura. Model je pripremljen i rešen primenom programskog paketa MSC/NASTRAN SOL103. Metodom dizajna eksperimenta identifikovani su kritični parametri, što je kasnije omogućilo dobijanje visokih MAC vrednosti.*

Ključne reči: *SDDTools-MATLAB, NASTRAN, modalna analiza, kompozitni materijali*